Integrated Cascaded Bragg Gratings for On-Chip Optical Delay Lines

Lingjun Jiang and Zhaoran Rena Huang

Abstract—We have demonstrated on-chip optical delay lines that consist of cascaded Bragg grating segments. Our results show that the band gap and the group index of cascaded gratings are very similar to that of a single grating segment, which means longer time delay can be achieved by cascading more grating segments. In our experiment, a maximum group index of 12.2 and a total time delay of 292 ps was achieved using a 7.2 mm-long delay line on Si chip.

Index Terms—Delay line, Bragg grating, integrated optics, slow light devices.

I. INTRODUCTION

INTEGRATED optical true delay line is one of the key elements used in many optical systems for time alignment or control of optical path length such as control of beam forming in phase array antennas (PAA) [1], and optical reservoir computing [2]. At present, long optical delays are mainly realized using fiber spools of different lengths. The advancement in Si photonics last decade has made it possible to integrate low-loss, long optical delay structures on Si chip.

Various photonic structures have been explored to make integrated Si-based optical delay lines. Resonant devices such as coupled-ring optical waveguides (CROWs) [3] and slow light based photonic crystal (PhC) waveguide [4] have been demonstrated. Integrated chirped Bragg grating is another kind of slow-light structure that has been demonstrated to realize large on-chip temporal delays [5], [6] due to its advantage of continuous tunability.

Apodized Bragg grating is an appealing alternative to construct on-chip time delay [7], particularly for applications that are in favor of wavelength dispersion [1], [2]. In practice, each Si chip has a finite dimension. For example, a unit area of 6×8.5mm surface area is defined by AIM manufacturing. To achieve delay of nanoseconds or even microseconds, a single element of grating waveguide is often not sufficient. Connecting multiple Bragg grating delay line elements is a practical solution to achieve long on-chip time delay.

Fabry-Perot (FP) effect in cascade grating segments has been reported in [8]. In this letter, we have designed and
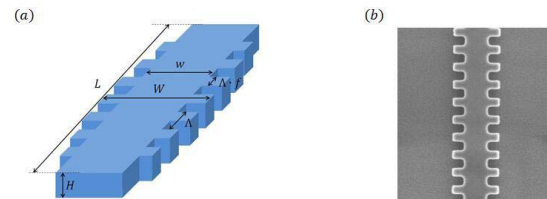
Fig. 1. (a) Schematic of a single element sidewall Bragg grating, (b) a SEM image of a portion of a fabricated Bragg grating on Si substrate.

demonstrated 2-segment and 4-segment optical delay lines to study the reflection, transmission and group index of cascaded Bragg grating waveguides.

II. DESIGN AND FABRICATION

Our structure is based on a sidewall Bragg grating, as shown in Fig. 1(a). The slow light effect originates from the forward and backward propagation of the light wave due to the reflection from the corrugated sidewalls. Since the sidewall exhibits periodicity with a fixed pitch size, the reflection caused by propagation wave resonance is wavelength dependent, which is the source of dispersion and can be utilized to realize enhanced true-time group delay. Super Gaussian function is a higher-order version of the Gaussian function, and is used to gradually modulate the coupling coefficient $\kappa(z)$ as light penetrates or exits the grating along the propagation direction. The apodization function is $f = \exp(-\frac{(z-L/2)^n}{2 \times \alpha^n})$, where L is the grating length, and the parameter α and n determine how smooth the transition is and are chosen to be 0.35 and 8, respectively. Other α and n combinations are also explored and they all show effectiveness in suppressing oscillations in the pass band of the grating transmission. In theory, tradeoff exists between the group index and the side band oscillation: a large n and α gives rise to greater true-time delay but stronger oscillations. The devices are fabricated on a SOI substrate with a top silicon layer of 250nm. A 3-dimensional finite-difference time domain (FDTD) simulation is performed to determine the device parameters, which are chosen as pitch size $\Lambda = 292$ nm, W = 800 nm, w = 400 nm, H = 250 nm, and a duty cycle f = 0.5. L is either 1.8 mm or 3.6 mm. Estimated from the Bragg condition, the effective index of the fundamental mode n_{eff} is 2.55. The maximum effective index modulation is $\delta n_{eff} = 0.058$, and it tapers down to 0 at the two facets due to apodization. Thus, the modulation amplitude is 0.058/2.55 = 0.023, cor-
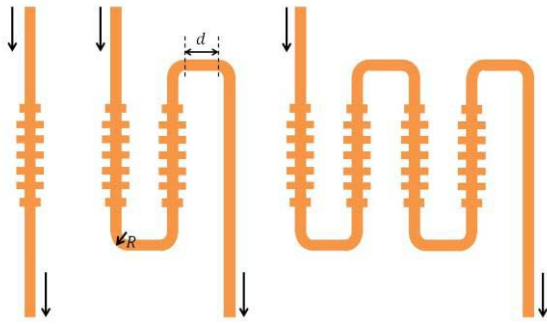
Fig. 2. Schematic of fabricated delay lines with 1, 2 and 4 grating segments cascaded.

responding to a $\Delta\lambda \sim 35$ nm reflection bandwidth with the Bragg wavelength of $\lambda = 1530$ nm. The design has been verified numerically by the FDTD simulation and later confirmed experimentally. A SEM image of a portion of a fabricated grating is shown in Fig. 1(b).

A schematic of cascaded gratings consisting of 1, 2 and 4 grating segments is shown in Fig. 2. Each segment in the cascaded configuration is identical and has a complete apodized grating function. The turning radius of the connecting waveguide is R $= 8$ μm and the separation between delay lines is d $= 2$ μm. A compact design can be achieved by reducing R, and the bending loss is very low even when the radius R is as small as 1 μm [9].

A C-band tunable laser with resolution of 1 GHz (or 0.008 nm) is used in the testing. The laser is connected to a polarization controller. Light is then coupled in and out the device through lensed fibers, and is sent into an optical spectrum analyzer (OSA) for optical power measurement. The Bragg grating is polarization-dependent since the rib waveguide has different effective index for TE and TM polarizations; and in our design TE mode is used.

III. EXPERIMENTAL RESULTS AND DISCUSSION

A. Transmission Spectrum

We first measure the transmission spectrum of the grating delay line with 1, 2 and 4 cascaded segments; and each segment is 3.6 mm long. The results are plotted in Fig. 3. The band edge of the single segment is at $\lambda \sim 1549$ nm, while band edges of the cascaded segments are both at $\lambda \sim 1547.5$ nm. This small variation can attribute to fabrication inaccuracy, i.e. small change in duty cycle as the e-beam lithography tool condition drifts during exposure. Quantitatively, a duty cycle decreases from 0.5 to 0.499 results in the shift of the band edge to a shorter wavelength by 1.5 nm.

The extinction ratio between the pass band and stop band is over 25 dB for all three devices, indicating strong reflections in the stop band. From the plots, the optical loss in the slow-light pass band regions of all three devices is almost the same. It implies that reflection loss from the apodized grating segment is minimal. The primary loss mechanism in our test is the coupling loss at the chip facets ($\sim$10 dB/facet).
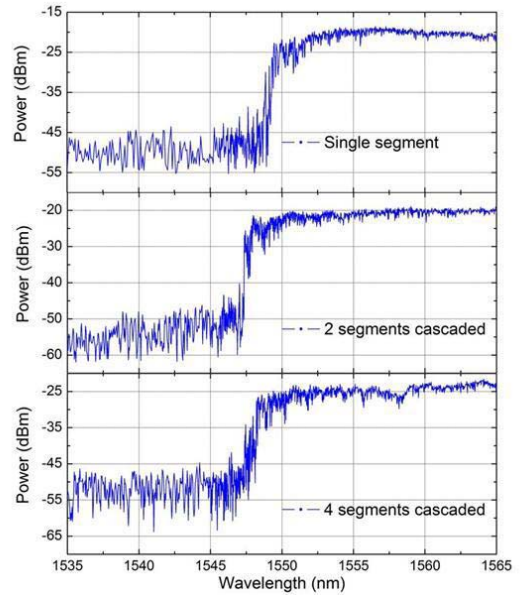

Fig. 3. Transmission spectrum of delay lines with 1, 2 and 4 grating segments cascaded.

FP resonance inevitably exists between segments as long as reflection isn't zero. As each grating segment in the Fig. 2 is 3.6mm, the apodization function has made an effective mode coupling from straight waveguide to slow-light grating waveguide, and thus the reflection is minimized. Numerical study has shown that a short segment, such as 100 periods ($\sim$30 μm) with the same apodization function has exhibits much increased reflectivity, and therefore much pronounced FP resonance between segments. However, the oscillatory behavior, especially the side-lobes in the vicinity of the band gap, is still visible. This is due to the reflections arising from the Bragg condition itself make it difficult to thoroughly remove all the FP noise. Also, the reflections at chip facets contribute to the overall FP noise as well.

B. Group Index and Total Delay

In order to measure group index, we follow the method in [10] by incorporating each of these gratings in a Mach-Zehnder interferometer (MZI). The signal arm of the MZI contains the grating waveguide to be measured, and the reference arm contains a grating waveguide of the same length, same apodization and a pitch size of 288 nm. Fig. 4(a) shows the transmission spectrum and the MZI measurement result of the delay line with two 1.8 mm-long segments cascaded. The transmission in red curve shows the band edge at $\lambda = 1548$ nm, while the interference fringes of the MZI (blue curve) is cut off at about $\lambda = 1549$ nm. At wavelengths between 1535 nm and 1549 nm, the MZI spectrum shows a strong oscillation noise, which is due to the reflections from the parasitic FP cavities in the optical path.

The group index n_g is extracted from the spectrum and plotted in Fig. 4(b). At $\lambda = 1549$ nm, the maximum extracted n_g is 12.2, corresponding to a time delay of 41 ps/mm. The n_g of the reference grating is $\sim$5 for the wavelength
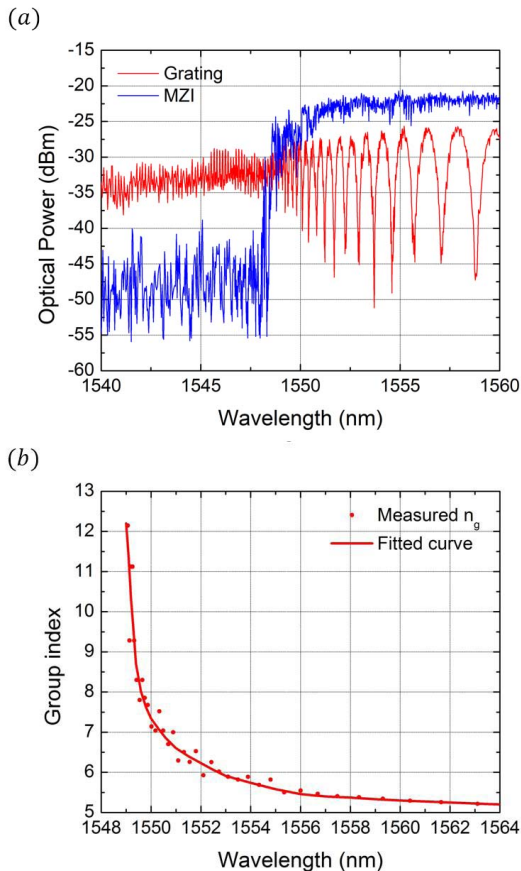
(a)

(b)

Fig. 4. (a) Measurement for delay line with 2 cascaded segments with MZI method, (b) Extracted group index.

range of interest based on our previous measurement. Therefore, the total time delay for the 3.6 mm-long delay line is about 148 ps. It's worth noting that between the wavelength of 1548 nm and 1549 nm, the delay line is still in the pass band, but n_g cannot be extracted due to the presence of FP noise in the interference fringe curve. This is the limitation of the MZI method to measure time delay. A higher group index is expected for wavelength between 1548-1549 nm. As modern lasers (such as Santec TSL-710) can achieve line width of ~ 100 kHz ($\sim 10^{-6}$ nm), it is plausible to operate the delay line device very close to the band edge for increased time delay per unit length.

In order to evaluate whether the cascaded multiple grating segments as a delay line can keep the same group index as a single grating segment, a group of devices are measured and compared. Fig. 5 plots the n_g measured for 4 delay lines, which are 3.6 mm $\times$ 2, 1.8 mm $\times$ 4, 3.6 mm $\times$ 1 and 1.8 mm $\times$ 2, respectively. The result shows that the n_g spectrum of these delay lines can mostly overlap with each other at $\lambda > 1552$ nm. At 1549 nm $< \lambda <$ 1552 nm, n_g of the 1.8 mm $\times$ 4 delay line cannot be extracted due to background spectrum noise, and the highest extracted n_g is 12.2 for the 1.8 mm $\times$ 2 delay line at $\lambda = 1549$ nm. From Fig. 4 (a), it can be seen that the band gap edge is at $\lambda = 1548$ nm, which means the actual maximum n_g is higher than 12.2. Using n_g of 12.2 for estimation, the 7.2 mm-long delay line has a total time delay of 292 ps.
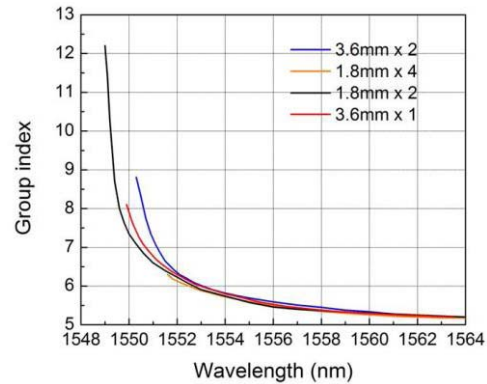

Fig. 5. Group index comparison of 4 cascaded on-chip optical delay lines.

C. Discussions

The integrated delay line of 3.6mm $\times$ 2 segments consumes a surface area of 4×0.03mm^2 and provides an estimated delay of 292 ps at $\lambda = 1549$ nm. To reduce the propagation loss of the delay lines, low loss SiN on Si waveguide can be used [11].

The cascading method to realize long time delay comes at a price. There is a universal trade-off between group delay and bandwidth due to dispersion-induced pulse broadening. Since the gratings are highly dispersive, the pulse broadening may degrade the signal integrity during transmission and thus lowering the bit rate of the channel. The length of the grating needs to be minimized in order to keep the pulse broadening under control. The maximum achievable delay is thus determined by the required date rate of the application [12]. Dispersion compensation or active approach [13] can be employed to reduce dispersion while keeping high group index. For applications that do not require high bit rate (<1 Gb/s), cascading delay line is still a practical solution to achieve long true time delay.

The MZI method has certain limitations. There are a number of parasitic FP resonance observed in the spectrum and they add oscillations to the n_g-λ curve. The source of the FP resonance includes reflections between the chip facets, splitters of the MZI, and the interface between grating and waveguide. Directional couplers have replaced the Y splitters in the MZI configuration. The apodization can substantially improve the mode coupling efficiency from the straight waveguide to the slow light grating, and thus effectively suppress the reflections at the grating/waveguide interface. For future work, we will consider real time measurement to characterize the wavelength-dependent delay time.

IV. CONCLUSION

In summary, we have explored the concept and physics of integrated optical delay lines using cascaded multiple grating segments to extend the total delay time. The group index of cascade grating is very close to that of a single grating segment with the same length. No strong FP cavity effect was observed between adjacent grating segments. A maximum group index of 12.2 and a total time delay of 292 ps has been achieved for a 7.2 mm-long cascaded grating delay lines with the consumption of a chip surface area of 4×0.03 mm^2.

References

[1] W. Zhou *et al.*, "Developing an integrated photonic system with a simple beamforming architecture for phased-array antennas," *Appl. Opt.*, vol. 56, no. 3, pp. B5–B13, 2017.

[2] Y. Paquot *et al.*, "Optoelectronic reservoir computing," *Sci. Rep.*, vol. 2, Feb. 2012, Art. no. 287.

[3] F. Morichetti, A. Melloni, A. Breda, A. Canciamilla, C. Ferrari, and M. Martinelli, "A reconfigurable architecture for continuously variable optical slow-wave delay lines," *Opt. Exp.*, vol. 15, no. 25, pp. 17273–17282, 2007.

[4] A. Melloni *et al.*, "Tunable delay lines in silicon photonics: Coupled resonators and photonic crystals, a comparison," *IEEE Photon. J.*, vol. 2, no. 2, pp. 181–194, Apr. 2010.

[5] D. T. H. Tan, K. Ikeda, R. E. Saperstein, B. Slutsky, and Y. Fainman, "Chip-scale dispersion engineering using chirped vertical gratings," *Opt. Lett.*, vol. 33, no. 24, pp. 3013–3015, 2008.

[6] V. Italia, M. Pisco, S. Campopiano, A. Cusano, and A. Cutolo, "Chirped fiber Bragg gratings for electrically tunable time delay lines," *IEEE J. Sel. Topics Quantum Electron.*, vol. 11, no. 2, pp. 408–416, Mar. 2005.

[7] S. Khan and S. Fathpour, "Demonstration of tunable optical delay lines based on apodized grating waveguides," *Opt. Exp.*, vol. 21, no. 17, pp. 19538–19543, 2013.

[8] S. Deng and Z. R. Huang, "Design and analysis of transmission enhanced multi-segment grating in MZI configuration for slow light applications," *Opt. Exp.*, vol. 19, no. 8, pp. 7872–7884, 2011.

[9] Y. A. Vlasov and S. J. McNab, "Losses in single-mode silicon-on-insulator strip waveguides and bends," *Opt. Exp.*, vol. 12, no. 8, pp. 1622–1631, Apr. 2004.

[10] Y. A. Vlasov, M. O'boyle, H. F. Hamann, and S. J. McNab, "Active control of slow light on a chip with photonic crystal waveguides," *Nature*, vol. 438, pp. 65–69, Nov. 2005.

[11] H. J. R. Martijn, J. F. Bauters, M. L. Davenport, D. T. Spencer, and J. E. Bowers, "Ultra-low loss waveguide platform and its integration with silicon photonics," *Laser Photon. Rev.*, vol. 8, no. 5, pp. 667–686, 2014.

[12] J. E. Sipe, B. J. Eggleton, and T. A. Strasser, "Dispersion characteristics of nonuniform Bragg gratings: Implications for WDM communication systems," *Opt. Commun.*, vol. 152, nos. 4–6, pp. 269–274, 1998.

[13] Q. Xu, P. Dong, and M. Lipson, "Breaking the delay-bandwidth limit in a photonic structure," *Nature Phys.*, vol. 3, pp. 406–410, Nov. 2007.